



Computer Aided Design Analysis of Electrical Motor Drives for Traction Application.

B.Ravikumar¹, Dr.Y.R.Manjunath²

Research Scholar, Dept. of EEE, Bangalore University, Bangalore, Karnataka, India

Professor, Dept. of EEE, Bangalore University, Bangalore, Karnataka, India

ABSTRACT: Strict environmental regulations and shrinkage of fossil fuel supplies necessitate the generation of electricity by using renewable energy sources. Most promising and popular source of green electricity is wind energy. WECS using DFIG is a meritorious option as it uses back to back power converters at a reduced rating, offers high controllability, allows maximum power extraction and individual control of active and reactive power components. As per modern grid rules, DFIG needs to operate without losing synchronism called low voltage ride through (LVRT) during severe grid faults. Hence, an enhanced field oriented control technique (EFOC) was adopted in Rotor Side Converter (RSC) of DFIG with PI and PI-Resonant Controller separately to improve the power flow transfer and to improve dynamic and transient stability and the corresponding results are studied. This paper mitigates voltage and limits surge currents to enhance the operation of DFIG during symmetrical and asymmetrical faults. The system performance with different types of grid faults like single line to ground, double line to ground and triple line to ground were applied with PI and PIR controller separately and the corresponding waveforms are presented by using MATLAB/Simulink software.

KEYWORDS: DFIG Doubly Fed Induction Generator, EFOC Enhanced Field Oriented Control, LVRT Low Voltage Ride Through, WECS Wind Energy System.

I. INTRODUCTION

As the wind power is increasingly penetrated into the grid, some new grid codes are proposed to improve power system stability [1], [2]. The new codes require wind energy conversion system (WECS) not only to remain connected to the grid, but also to inject reactive current into the grid for restoring the grid voltage during grid faults. A doubly fed induction generator (DFIG)-based wind turbine (WT) is an economical choice for wind farms, because it reduces the cost and power loss [3], [4]. is directly connected to the grid, the DFIG is sensitive to grid disturbances and faults, and it is also difficult to fulfill low-voltage ride through (LVRT) requirements. The methods to improve the LVRT ability of the DFIG may into two main categories, namely, auxiliary hardware circuit method and improved control strategy. The auxiliary hardware circuit normally includes rotor crowbar circuit [5], [6], dynamic voltage restorer (DVR) [7], [8], series stator side impedance network [9], [10], series grid side converter (SGSC) [11], [12], and dc-link chopper [13]. The rotor crowbar circuit is the most popular method to fulfill LVRT requirement by shorting the rotor windings during grid faults. When the rotor windings are shorted, the DFIG works as a conventional squirrel-cage induction motor and absorbs reactive power from the grid [5], [6]. The methods of DVR [7], [8] and SGSC [11], [12] fulfilled LVRT requirement by compensating the terminal voltage of the stator during grid faults. Therefore, the LVRT ability is strongly dependent on the capacities of the series converter and transformer. The method with series impedance network in the terminal of the stator winding may reduce the transient period and suppress the rotor current during grid faults. But it requires that the parameters of the impedance network are equal to the sum of the equivalent parameters of the grid and the generator [10]. As the impedances are connected in series and parallel with the stator windings during grid faults, the stator power will flow through the resistances, and produce power loss and extra heat. Furthermore, the parameters of DFIG and DFIG connected grid need to be measured or estimated, which may increase the complexity. Although these methods with the auxiliary hardware circuits can fulfill LVRT requirement, the size, weight, and cost of the WECS are increased, which sacrifice the merit of the conventional DFIG-based WECS with a partial rated power converter. Several studies have also been proposed to suppress rotor current during grid faults by improving

International Journal of Advanced Research in Electrical, Electronics and Instrumentation Engineering

(An ISO 3297: 2007 Certified Organization)

Vol. 4, Issue 12, December 2015

control strategies for the rotor side converter (RSC). A fast response vector-based hysteresis current controller was used to achieve DFIG LVRT Requirement [14], [15]. By limiting output of stator active power to reduce rotor currents during grid faults was proposed in [16] and [17]. This method works well under steady state and [16] Improves [17] by injecting reactive power into the grid. These methods achieve LVRT requirement by only improving the dynamic response of the control system or limiting the output powers, but do not damp the stator flux. Therefore, the DFIG may become uncontrollable, and the rotor may suffer from Over-current under some conditions. The stator flux may include positive and negative sequence components, as well as transient component during grid faults [18]. The stator flux-based control strategies were proposed to fulfill LVRT requirement in [19]–[21]. In [20], a virtual

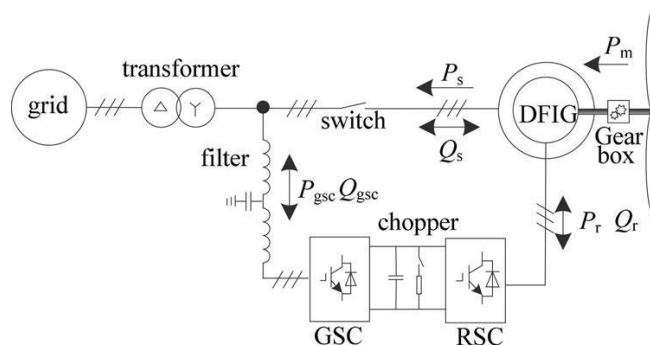


Fig. 1. Structure diagram of a DFIG-based WECS.

resistance was used to improve the control strategy presented in [19] by increasing the damping ratio so that the transient flux can decay fast. However, during asymmetrical grid faults, the control of the negative sequence stator flux is not as important as the transient stator flux, because it cannot disappear like the transient flux. The control of negative sequence flux may slow the decaying speed of the transient flux, and increase the rotor current amplitude. Moreover, the electromagnetic torque is fluctuant during grid faults. On the other hand, it is difficult to improve the performances of DFIG during unbalanced grid faults [19], [20]. In [21], a flux linkage tracking control strategy was proposed for DFIG to achieve LVRT requirement. However, the reactive power required by grid code is not involved. Reduction of torsional oscillation as the control target was introduced to improve DFIG performances during asymmetrical grid fault, but the influence of magnetic nonlinearity characteristic is not considered in [22]. When the grid voltage is unbalanced, considering the magnetic nonlinearity characteristics, the grid connected DFIG may be regarded as an equivalent circuit with unbalanced power source and unbalanced load. Then, the performance of DFIG is degraded.

In this paper an enhanced field oriented control technique (EFOC) was adopted in Rotor Side Converter of DFIG converter to improve dynamic and transient stability. For the EFOC technique, rotor flux reference changes its value from synchronous speed to zero during fault for injecting current at the rotor slip frequency. In this process DC-Offset component of flux is controlled, decomposition during symmetric and asymmetric faults. The offset decomposition of flux will be oscillatory in a conventional field oriented control, whereas in EFOC it was aimed to damp quickly. This paper mitigates voltage and limits surge currents to enhance the operation of DFIG during symmetrical and asymmetrical faults. By using PI Controller and PIR Controller in RSC separately the system performance with different types of faults like single line to ground, double line to ground and triple line to ground were applied and the corresponding waveforms are studied.



International Journal of Advanced Research in Electrical, Electronics and Instrumentation Engineering

(An ISO 3297: 2007 Certified Organization)

Vol. 4, Issue 12, December 2015

II. DFIG PERFORMANCES

The structure diagram of the DFIG-based WECS is shown in Fig. 1. In the stationary reference frame, the DFIG voltage and flux equations, in the form of vector, are expressed as

$$\begin{aligned}
 u_s &= R_s i_s + p \phi_s \\
 u_r &= R_r i_r + p \phi_r + j \omega_r \phi_r \\
 \left\{ \begin{array}{l} \phi_s = L_m i_r + L_s i_s \\ \phi_r = L_r i_r + L_m i_s \end{array} \right.
 \end{aligned} \quad (1)$$

where u , i , and ϕ are the vectors of voltage, current, and flux, respectively, R is the resistance, and L is the inductance. Subscripts “s” and “r” distinguish the stator and rotor variables. Superscript “s” represents the stationary reference frame. L_m is the mutual inductance, p stands for the differential operator, and ω_r is the rotor electrical frequency.

Replacing the stator current with stator flux and rotor current, the stator voltage equation in (1) is re-expressed as

$$p \phi_s = u_s - \frac{R_s}{L_s} \phi_s - \frac{m}{L_s} i_r \quad (2)$$

The rotor current may be expressed as

$$i_r = \frac{1}{R_r} \left(u_r - p \phi_r \right) \quad (3)$$

where $\phi_r = a \tan(i_r)$, $I_r = \sqrt{2} i_r$, “d” and “q”

$$\begin{aligned}
 & \text{represent d and q-axes components, respectively, in the synchronous reference frame.} \\
 & \text{In Fig. 1, due to a wye-delta isolation transformer, during asymmetrical grid faults, the stator voltage may only include positive and negative sequence components and be expressed as}
 \end{aligned}$$

$$\begin{aligned}
 u_s &= u_s + u_s \\
 &= e^{j\omega t} U_{sm} + e^{j\omega t} U_{sn} \quad (4)
 \end{aligned}$$



International Journal of Advanced Research in Electrical, Electronics and Instrumentation Engineering

(An ISO 3297: 2007 Certified Organization)

Vol. 4, Issue 12, December 2015

$$U_{sm}$$

where superscripts “+” and “-” represent positive and negative sequence components, respectively. U_{sm} represents voltage amplitude.

By substituting (3) (4) into (2), it results in

$$\frac{d\psi_s}{dt} + \frac{R_s}{L_s} \psi_s = U_s^+ e^{j\omega_s t} + U_s^- e^{-j\omega_s t} + C e^{-\frac{t}{L_s R_s}} \quad (5)$$

where $L_s R_s$ is the stator time constant and C is the initial amplitude of the transient stator flux.

On the right side of (5), the first term is the transient component of stator flux, and the other three terms are steady-state components of stator flux. During grid voltage drop and recovery, the stator transient component may exist, while in the steady state, it is equal to zero.

Given that a grid fault occurs at t_0 , the stator voltage is expressed as

$$\vec{u}_s = \begin{cases} U_{sm1}^+ e^{j\omega_s t} + U_{sm1}^- e^{-j\omega_s t}, & t \leq t_0 \\ U_{sm2}^+ e^{j\omega_s t} + U_{sm2}^- e^{-j\omega_s t}, & t > t_0 \end{cases} \quad (6)$$

where subscripts “1” and “2” distinguish the values before and after grid fault. If the grid voltage is balanced, the negative sequence component of the stator voltage is equal to zero.

The corresponding stator flux is then expressed as

$$\vec{\psi}_s = \begin{cases} C_1 e^{-\frac{t}{\tau}} + \frac{\vec{u}_{s1}^+}{j\omega_s + \frac{1}{\tau}} + \frac{\vec{u}_{s1}^-}{-j\omega_s + \frac{1}{\tau}} - \frac{L_m R_s \vec{i}_r^s}{L_s j\omega_s + \frac{1}{\tau}}, & t \leq t_0 \\ C_2 e^{-\frac{(t-t_0)}{\tau}} + \frac{\vec{u}_{s2}^+}{j\omega_s + \frac{1}{\tau}} + \frac{\vec{u}_{s2}^-}{-j\omega_s + \frac{1}{\tau}} - \frac{L_m R_s \vec{i}_r^s}{L_s j\omega_s + \frac{1}{\tau}}, & t > t_0 \end{cases} \quad (7)$$



International Journal of Advanced Research in Electrical, Electronics and Instrumentation Engineering

(An ISO 3297: 2007 Certified Organization)

Vol. 4, Issue 12, December 2015

As the stator flux is a state variable and continuous at t_0 , if rotor current is under control, from (7), it is obtained that

$$C_2 e^{-\frac{(t-t_0)}{\tau}} = C_1 e^{-\frac{t_0}{\tau_s}} + \frac{(U_{sm1}^+ - U_{sm2}^+) e^{j\omega_s t_0}}{j\omega_s + 1/\tau} + \frac{(U_{sm1}^- - U_{sm2}^-) e^{-j\omega_s t_0}}{-j\omega_s + 1/\tau}. \quad (8)$$

In (8), it can be seen that C_2 is not only determined by the instants and depths of voltage variations, but also the amplitude of the transient flux $C_1 e^{-\frac{t_0}{\tau_s}}$, which is the first term on the right of (8). Therefore, if the transient flux is equal to zero at t_0 , it may avoid the amplitude of the new transient flux $C_2 e^{-\frac{(t-t_0)}{\tau}}$ being too large.

By replacing the rotor flux with stator flux and rotor current, the rotor voltage equation in (1) may be re-expressed as

$$\vec{u}_r^s = R_r \vec{i}_r^s + \frac{L_s}{L_m} p \vec{\varphi}_s^s + \sigma L_r p \vec{i}_r^s - j\omega_r \left(\frac{L_s}{L_m} \vec{\varphi}_s^s + \sigma L_r \vec{i}_r^s \right). \quad (9)$$

If the rotor current is equal to zero, (9) may be re-expressed as

$$\vec{u}_{r0}^s = \frac{L_m}{L_r} p \vec{\varphi}_s^s - j\omega_r \frac{L_m}{L_r} \vec{\varphi}_s^s. \quad (10)$$

When rotor current is equal to zero, from (2), it may be derive that

$$\frac{L_m}{L_r} (p \vec{\varphi}_s^s - j\omega_r \vec{\varphi}_s^s) = \frac{L_m}{L_r} \left(\vec{u}_s^s - \left(j\omega_r + \frac{R_s}{L_s} \right) \vec{\varphi}_s^s \right). \quad (11)$$

By substituting (5) into (11), it results in

$$\vec{u}_{r0}^s = \frac{L_m}{L_r} \left(\vec{u}_s^s - \left(j\omega_r + \frac{R_s}{L_s} \right) \times \left(C e^{-\frac{1}{\tau} t} + \frac{\vec{u}_s^{s+}}{j\omega_s + \frac{1}{\tau}} + \frac{\vec{u}_s^{s-}}{-j\omega_s + \frac{1}{\tau}} \right) \right). \quad (12)$$



International Journal of Advanced Research in Electrical, Electronics and Instrumentation Engineering

(An ISO 3297: 2007 Certified Organization)

Vol. 4, Issue 12, December 2015

In (12), if the module of \vec{u}_s is larger than the maximum
 u_{r0}

amplitude supplied by the RSC, the rotor current may become uncontrollable, which may potentially destroy the RSC. Therefore, the stator flux may cause the DFIG to be out of control. A possible way to reduce the module of \vec{u}_s is to reduce u_{r0}

the amplitude of the transient component, because the positive and negative sequence voltages are directly determined by the

grid. From (8), when grid voltage varies at t_0 , if \vec{u}_s is not equal to zero, it may lead to a large transient flux $C_2 e^{\lambda(t-t_0)}/\lambda$.

Therefore, if a strategy can suppress the transient flux fast, the rotor over-current may be avoided.

The electromagnetic torque is expressed as

$$T_e = -\frac{3}{2} n_p \text{Im}(\vec{\varphi}_s^* \times \vec{i}_s^*) \quad (13)$$

where superscript “^” represents conjugation of vector. The stator active and reactive powers are expressed as

$$S = P_s + jQ_s = -\frac{3}{2} \vec{u}_s^* \times \vec{i}_s^* \quad (14)$$

III. PROPOSED CONTROL STRATEGIES

A. ENHANCED FIELD ORIENTED CONTROL

The field orientation techniques allow decoupled or independent control of both active and reactive power. These techniques are based on the concept of $d^e - q^e$ controlling in different reference frames, where the current and the voltage are decomposed into distinct components related to the active and reactive power. In this work, the stator flux oriented rotor current control, with decoupled control of active and reactive powers is adopted.

The control schemes for the doubly-fed induction machine are expected to track a prescribed maximum power curve, for maximum power capturing and to be able to control the reactive power generation. These control objectives must be achieved with adequate stability of the system which also includes the power converter and the dc link.

$$P_s = \frac{3}{2} |V_s| i_{qs}^e \quad (15)$$

$$Q_s = \frac{3}{2} |V_s| i_{ds}^e \quad (16)$$

$$Q_s = \frac{3}{2} |V_s| i_{ds}^e$$



International Journal of Advanced Research in Electrical, Electronics and Instrumentation Engineering

(An ISO 3297: 2007 Certified Organization)

Vol. 4, Issue 12, December 2015

Where $|V_s| \approx \sqrt{(V_{ds}^e)^2 + (V_{qs}^e)^2}$

The field orientation control is based on the field $d^e - q^e$ model, where the reference frame rotates synchronously with respect to the stator flux linkage, with the d-axis of the reference frame instantaneously overlaps the axis of the stator flux. By aligning the stator flux phasor λ_s on the d^e - axis, so ($\omega = \omega_e$ and $\lambda_{qs}^e = 0, s e ds \lambda_{ds}^e = \lambda_s$). In such case the following expressions are obtained

$$\lambda_{qs}^e = L_s i_{qs}^e + L_m i_{qr}^e = 0.0$$

$$\therefore i_{qs}^e = -\frac{L_m}{L_s} i_{qr}^e$$

The developed electromagnetic torque can be expressed in terms of $d^e - q^e$ stator current and flux components as:

$$T_e = \frac{3}{2} \frac{P}{2} (i_{qs}^e \lambda_{ds}^e - i_{ds}^e \lambda_{qs}^e)$$

By putting $\lambda_{qs}^e = 0$, in the torque equation, this yields:

$$\therefore T_e = \frac{3}{2} \frac{P}{2} (i_{qs}^e \lambda_{ds}^e) \tag{19}$$

Using (17) in and the active power equation (15), the equation of active power becomes

$$P_s = -\frac{3}{2} |V_s| \frac{L_m}{L_s} i_{qr}^e \tag{20}$$

21.

$$i_{ds}^e = i_{md}^e - i_{dr}^e = \frac{|V_s|}{2\pi f_s L_m} - i_{dr}^e$$

Using (21) and the reactive power equation (15), the equation of the reactive power can be expressed as follows:

$$Q_s = \frac{3}{2} |V_s| \left(\frac{|V_s|}{2\pi f_s L_m} - i_{dr}^e \right) \tag{22}$$



International Journal of Advanced Research in Electrical, Electronics and Instrumentation Engineering

(An ISO 3297: 2007 Certified Organization)

Vol. 4, Issue 12, December 2015

Therefore, the d^e -axis rotor current component, (i_{dr}^e) can be obtained by regulating the stator reactive power. On the other hand, the q^e -axis rotor current component, (i_{qr}^e) can be obtained by controlling the generated torque which is obtained from the stator active power and the generator speed.

The stator flux linkage components in the stationary stator reference frame can be calculated through the integration of the difference between the phase voltage and the voltage drop in the stator resistance as;

$$\begin{aligned}\lambda_{ds}^s &= \int (V_{ds}^s - i_{ds}^s R_s) dt \\ \lambda_{qs}^s &= \int (V_{qs}^s - i_{qs}^s R_s) dt\end{aligned}\quad (23)$$

The magnitude of the stator flux linkage and its phase angle are given by:

$$\begin{aligned}\lambda_s &= \sqrt{(\lambda_{ds}^s)^2 + (\lambda_{qs}^s)^2} \\ \theta_e &= \tan^{-1} \frac{\lambda_{qs}^s}{\lambda_{ds}^s}\end{aligned}\quad (24)$$

In Enhanced Field Oriented Control (EFOC) the direct and quadrature axis (d and q axis) currents are used to control effectively flux decay during symmetrical or asymmetrical faults. The rotor speed is multiplied with pole numbers and is subtracted from angular grid synchronous frequency. Later it is integrated and given a 90° phase shift to get rotor slip injection frequency angles (θ_s). At this slip frequency RSC converter injects current into the rotor circuit to control the rotor speed for optimum value and to control grid reactive power. The stator voltage magnitude is compared and controlled using PI or PIR controller to get the q-axis current. Similarly, rotor actual speed and optimal speed reference are controlled using PI or PIR to obtain the d-axis reference current. They are compared with an actual rotor d and q axis currents and controlled with tuned PI controllers to obtain the rotor injecting d and q axis voltages. The d and q voltages are converted into three-axis abc voltage using phase locked loop (PLL) within verse parks transformation and are given to a PWM pulse generator for obtaining pulses in the RSC converter. The flux derivation technique helps in understanding the operation of DFIG during steady state and transient state. The accuracy of system performance during steady state depends on the accuracy of wind speed measurement action of pitch angle controller, measurement of stator current, voltage, flux and other important parameters.

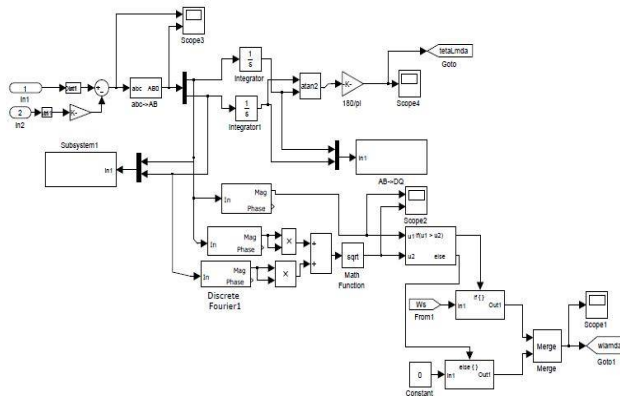


Fig. 2. MATLAB EFOC Subsystem in the RSC Controller.

B. PIR CONTROLLER

The positive- and negative-sequence currents must be controlled precisely in order to meet the control objectives. Good current control depends on the accuracy of the d - q components' decoupling and the removal of network voltage disturbance. Typical RSC (DFIG) and GSC control designs employ two current controllers implemented in the positive and negative synchronous reference frames, respectively [23], [24], [25]. However, the positive- and negative-sequence components of the currents have to be decomposed from measured signals involving time delay and resulting in amplitude and phase errors. Consequently, the systems cannot be fully decoupled during transients, degrading system performance and stability. In order to overcome these problems, the strategy adopted here is to have a PI-R current controller [26], [28], [27]. The R regulator has been widely presented as an interesting alternative in the stationary frame to the use of synchronous PI controllers [29]–[31], [28]. This regulator generally consists of a proportional and an integrator term, which contains an R pole, with the aim of obtaining an infinite gain at the R frequency. In order to reduce the sensitivity toward possible grid frequency variation, a component with a cutoff frequency of $\omega c1$ can be inserted into the R part to widen its frequency bandwidth, as shown in Fig. 3.

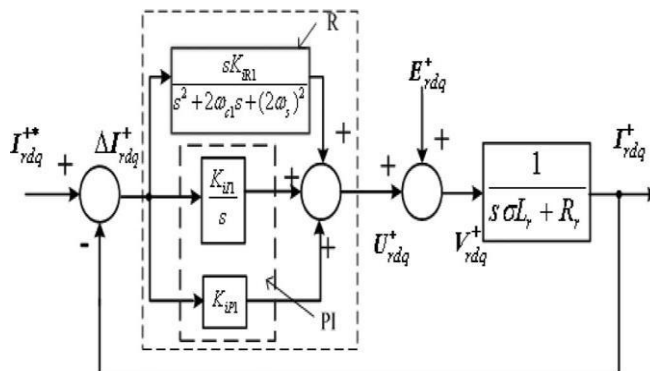


Fig.3. Rotor current control scheme based on PI-R controller in the $dq+$ reference frame.

In this paper, the PI-R controller is designed in the positive synchronous $dq+$ reference frame. Thus, the positive sequence voltage, current, and flux all become dc values, whereas the negative-sequence components appear as double-frequency ripples. With a PI-R controller, the dc components are mainly regulated by the PI controller while the double-frequency ac signals are fully controlled by the R regulator. Hence, a PI-R current controller in the positive synchronous



International Journal of Advanced Research in Electrical, Electronics and Instrumentation Engineering

(An ISO 3297: 2007 Certified Organization)

Vol. 4, Issue 12, December 2015

reference frame can directly regulate both positive- and negative-sequence components without involving sequential decomposition.

C. ASYMMETRICAL GRID FAULTS

When the grid voltage is unbalanced, the active and reactive powers may be expressed as

$$S = P_s + jQ_s = P_{s_A} + P_{s_B} + j(Q_{s_A} + Q_{s_B}) \quad (25) \text{ with}$$

$$\begin{aligned} P_{s_A} &= -\frac{3}{2}(u_{s\alpha}^{s+} i_{s\alpha}^{s+} + u_{s\beta}^{s+} i_{s\beta}^{s+} + u_{s\alpha}^{s-} i_{s\alpha}^{s-} + u_{s\beta}^{s-} i_{s\beta}^{s-}) \\ P_{s_B} &= -\frac{3}{2}(u_{s\alpha}^{s+} i_{s\alpha}^{s-} + u_{s\beta}^{s+} i_{s\beta}^{s-} + u_{s\alpha}^{s-} i_{s\alpha}^{s+} + u_{s\beta}^{s-} i_{s\beta}^{s+}) \\ Q_{s_A} &= -\frac{3}{2}(u_{s\beta}^{s+} i_{s\alpha}^{s+} - u_{s\alpha}^{s+} i_{s\beta}^{s+} + u_{s\beta}^{s-} i_{s\alpha}^{s-} - u_{s\alpha}^{s-} i_{s\beta}^{s-}) \\ Q_{s_B} &= -\frac{3}{2}(u_{s\beta}^{s+} i_{s\alpha}^{s-} - u_{s\alpha}^{s+} i_{s\beta}^{s-} + u_{s\beta}^{s-} i_{s\alpha}^{s+} - u_{s\alpha}^{s-} i_{s\beta}^{s+}) \end{aligned} + \frac{2}{3} \frac{L_s}{L_m} \left(\frac{P_{r_A}}{M_1} \begin{bmatrix} u_{s\alpha}^{s+} \\ u_{s\beta}^{s+} \\ u_{s\alpha}^{s-} \\ u_{s\beta}^{s-} \end{bmatrix} + \frac{Q_{r_A}}{M_2} \begin{bmatrix} -u_{s\beta}^{s+} \\ u_{s\alpha}^{s+} \\ u_{s\beta}^{s-} \\ -u_{s\alpha}^{s-} \end{bmatrix} \right)$$

where α and β represent the α and β -axes components in the stationary reference frame, respectively. The electromagnetic torque may be expressed as

$$T_e = T_{e_A} + T_{e_B} + E_T \quad (27)$$

with

$$\begin{aligned} T_{e_A} &= -\frac{3}{2} n_p (u_{s\alpha}^{s+} i_{s\alpha}^{s+} + u_{s\beta}^{s+} i_{s\beta}^{s+} - u_{s\alpha}^{s-} i_{s\alpha}^{s-} - u_{s\beta}^{s-} i_{s\beta}^{s-}) \\ T_{e_B} &= -\frac{3}{2} n_p (u_{s\alpha}^{s+} i_{s\alpha}^{s-} + u_{s\beta}^{s+} i_{s\beta}^{s-} - u_{s\alpha}^{s-} i_{s\alpha}^{s+} - u_{s\beta}^{s-} i_{s\beta}^{s+}) \\ E_T &= -\frac{3}{2} n_p R_s \left((i_{s\alpha}^{s+})^2 + (i_{s\beta}^{s+})^2 - (i_{s\alpha}^{s-})^2 - (i_{s\beta}^{s-})^2 \right) \end{aligned}$$

where n_p represents the pole pairs. P_{sA} , Q_{sA} in (29) and T_{eA} in (31) are the constant terms, and P_{sB} , Q_{sB} , and T_{eB} are fluctuant terms with two times of the fundamental frequency, and E_T is the power loss on the stator resistance. If $T_{eB} = Q_{sB} = 0$, the terms of the oscillation of the electromagnetic torque and reactive power may be suppressed. By setting $T_{e_B}/n_p = Q_{sB} = 0$ and P_{sA} , Q_{sA} are equal to their references, it leads to

International Journal of Advanced Research in Electrical, Electronics and Instrumentation Engineering

(An ISO 3297: 2007 Certified Organization)

Vol. 4, Issue 12, December 2015

$$\begin{bmatrix} P_{s_A} \\ Q_{s_A} \\ T_{e_B}/n_p \\ Q_{s_B} \end{bmatrix} = \begin{bmatrix} P_{s_ref} \\ Q_{s_ref} \\ 0 \\ 0 \end{bmatrix} = -\frac{3}{2} \begin{bmatrix} u_{s\alpha}^{s+} & u_{s\beta}^{s+} & u_{s\alpha}^{s-} & u_{s\beta}^{s-} \\ u_{s\beta}^{s+} & -u_{s\alpha}^{s+} & u_{s\beta}^{s-} & -u_{s\alpha}^{s-} \\ -u_{s\alpha}^{s-} & -u_{s\beta}^{s-} & u_{s\alpha}^{s+} & u_{s\beta}^{s+} \\ u_{s\beta}^{s-} & -u_{s\alpha}^{s-} & u_{s\beta}^{s+} & -u_{s\alpha}^{s+} \end{bmatrix}$$

$$\begin{bmatrix} u_{s\alpha}^{s+} \\ u_{s\beta}^{s+} \\ u_{s\alpha}^{s-} \\ u_{s\beta}^{s-} \end{bmatrix} = -\frac{3}{2} \left(\frac{P_{s_A}}{M_1} \begin{bmatrix} u_{s\alpha}^{s+} \\ u_{s\beta}^{s+} \\ u_{s\alpha}^{s-} \\ u_{s\beta}^{s-} \end{bmatrix} + \frac{Q_{s_A}}{M_2} \begin{bmatrix} -u_{s\beta}^{s+} \\ u_{s\alpha}^{s+} \\ u_{s\beta}^{s-} \\ -u_{s\alpha}^{s-} \end{bmatrix} \right)$$

where $M_1 = |u_{s\alpha}^{s+}|^2 + |u_{s\beta}^{s+}|^2$ and $M_2 = -|u_{s\alpha}^{s+}|^2 + |u_{s\beta}^{s+}|^2$.
Symbol “|” represents the vector module.

From the relationship between stator flux and currents, the rotor reference currents are expressed as

$$\begin{bmatrix} i_{r\alpha}^{s+} \\ i_{r\beta}^{s+} \\ i_{r\alpha}^{s-} \\ i_{r\beta}^{s-} \end{bmatrix} = \frac{1}{\omega L_m} \begin{bmatrix} u_{s\alpha}^{s+} \\ -u_{s\beta}^{s+} \\ -u_{s\alpha}^{s-} \\ u_{s\beta}^{s-} \end{bmatrix}$$

IV. SIMULATION RESULTS & DISCUSSION

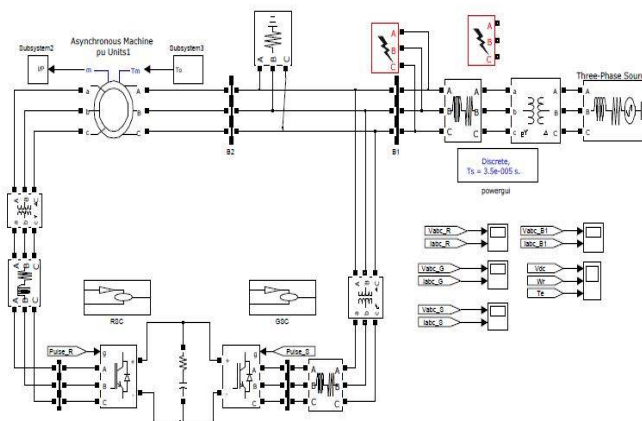


Fig.4. MATLAB based DFIG Model.

A. WITH PI CONTROLLER

In Fig. 4 the MATLAB based DFIG model circuit is shown with RSC and GSC controllers. The simulation is carried out in MATLAB/Simulink/Sim Power System software R2009b environment. In RSC initially PI Controller was used and fault was created at $t=0.6s$ to $0.8s$. The different faults are applied like LG, LLG, LLLG and the corresponding waveforms are shown in the Fig.5 to Fig.7 respectively. The figures indicate the terminal voltage and current of the DFIG during the pre-fault, during fault and post-fault.

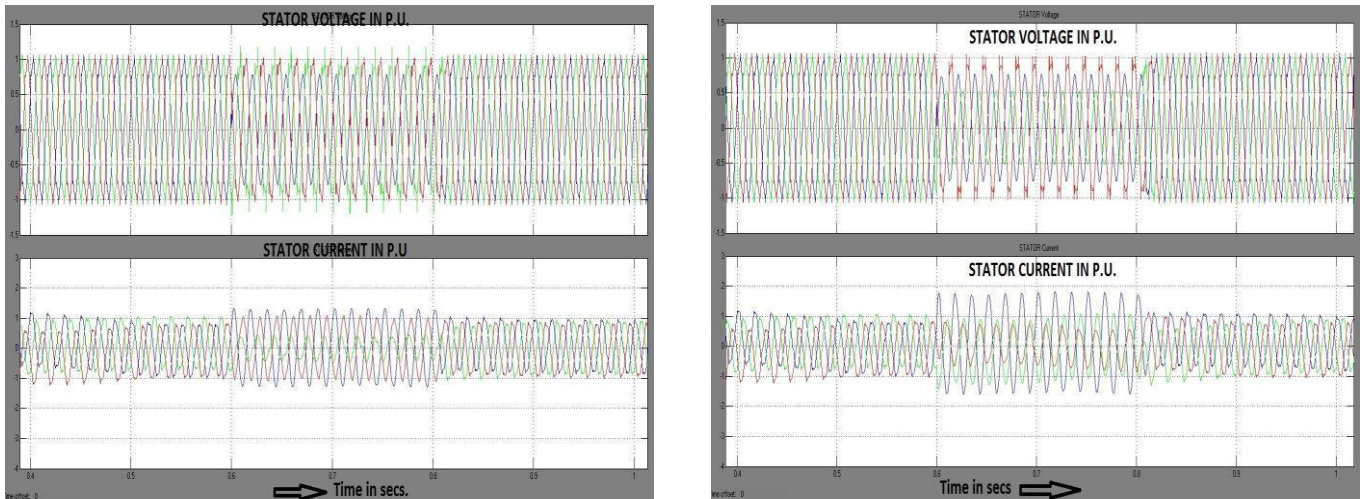


Fig.5. Simulation result of DFIG Performance with Terminal Voltage and current during a LG fault using a PI Controller.
Fig.6. Simulation result of DFIG Performance with Terminal Voltage and current during a LLG fault using a PI Controller

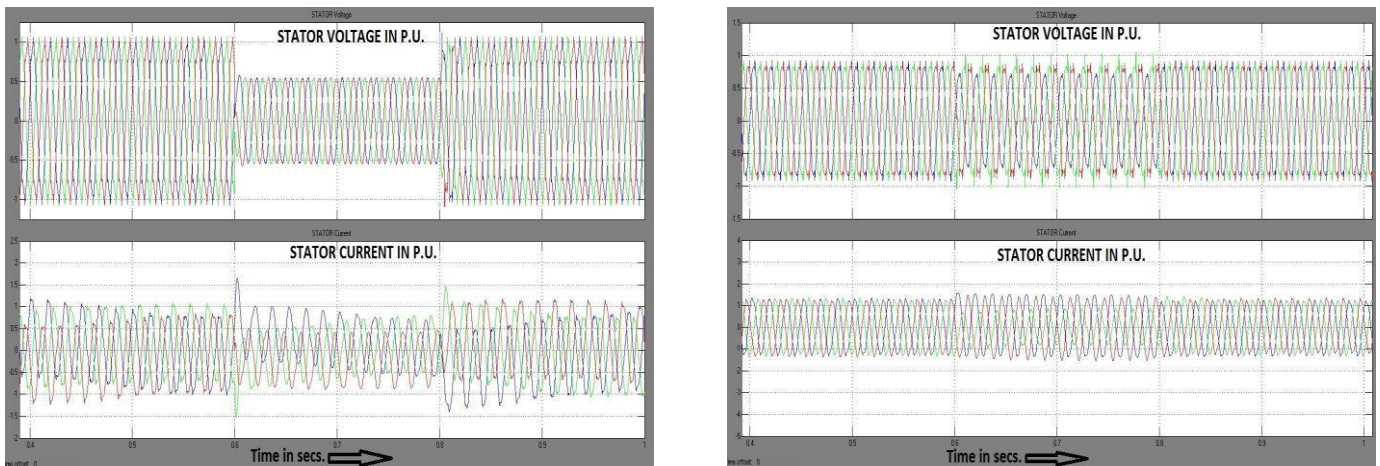


Fig.7. Simulation result of DFIG Performance with Terminal Voltage and current during a LLLG fault using a PI Controller.

Fig.8. Simulation result of DFIG Performance with Terminal Voltage and current during a LG fault using a PIR Controller.

B. WITH PI-RESONANT CONTROLLER

The Proportional and Integral (PI) Controller cannot suppress the steady-state error of the ac signal. Therefore, the rotor current is controlled by a proportional-integral-resonant controller, which can control not only dc signal with zero steady-state error, but also the ac signal with a high gain, as compared to the PI controller. PIR Controller was used in RSC and again faults are created at $t=0.6s$ to $t=0.8s$. The different faults are applied like LG, LLG, LLLG and the corresponding

International Journal of Advanced Research in Electrical, Electronics and Instrumentation Engineering

(An ISO 3297: 2007 Certified Organization)

Vol. 4, Issue 12, December 2015

waveforms are shown in the Fig.8 to Fig.10 respectively. The figures indicate the terminal voltage and current of the DFIG during the pre-fault, during fault and post-fault.

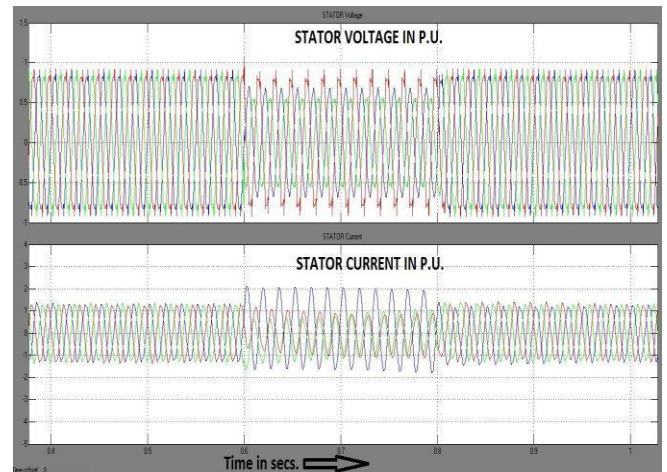
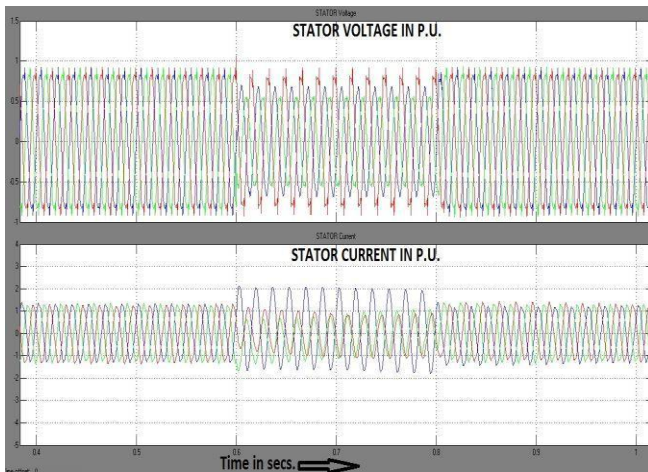


Fig.9. Simulation result of DFIG Performance with Terminal Voltage and current during a LLG fault using a PIR Controller.

Fig.10. Simulation result of DFIG Performance with Terminal Voltage and current during a LLLG fault using a PIR Controller.

V. CONCLUSION

A conventional DFIG system connected considered with three different faults like SLG, DLG and TLG are analyzed with PI Controller and PIR Controller separately. The three faults are imagined to occur at PCC between 0.6 and 0.8s with a fault resistance of 0.01 Ω . The drop in rotor and GSC terminal voltage during fault remained asymmetric faults and reached half for symmetric fault. With the proposed EFOC technique, rotor current during any fault did not reach zero in magnitude. Therefore, the whole system is to be disconnected from the grid during severe voltage dips but this is not acceptable by the new grid requirements, which require wind turbines to have LVRT capability and this was achieved in our paper.

APPENDIX

The parameters of DFIG used in simulation are:

Rated Power = 1.5MW,

Rated Voltage = 690 V,

Stator Resistance $R_s = 0.0049pu$,

Rotor Resistance $R_r1 = 0.0055pu$,

Stator Leakage Inductance $L_{ls} = 0.093 pu$,

Rotor Leakage inductance $L_{lr1} = 0.1pu$,

Inertia constant = 4.9 pu,

Number of poles = 4,

Mutual Inductance $L_m = 3.39 pu$,



International Journal of Advanced Research in Electrical, Electronics and Instrumentation Engineering

(An ISO 3297: 2007 Certified Organization)

Vol. 4, Issue 12, December 2015

DC link Voltage = 415V,

Grid frequency = 60 Hz.

Dc link capacitance = 0.2 F,

Wind speed = 14m/s.

Grid side Filter Rfg = 0.3 Ω ,

Lfg = 0.6 nH

Grid Voltage = 25 kV,

Transformer-690/440V, 50 kVA rating.

REFERENCES

- [1] "Technical regulation 3.2.5 for wind power plants with a power output greater than 11 kW," (Energinet.dk, Sept. 2010). [Online]. Available: <http://www.energinet.dk/EN/El/Forskrifter/Technical-regulation/s/Sider/Regulations-for-grid-connection.aspx>
- [2] "Grid Code High and Extra high voltage" (B. E. ON Netz GmbH, 2006, Apr.). [Online]. Available: http://www.pvupscale.org/MG/pdf/D4_2_DE_annex_A-3_EON_HV_grid_connection_requirements_ENENARHS2006de.pdf
- [3] S. Muller, M. Deicke, and R. W. De Doncker, "Doubly fed induction generator systems for wind turbines," IEEE Ind. Appl. Mag., vol. 8, no. 3, pp. 26–33, May/June 2002.
- [4] Petersson, T. Thiringer, L. Harnfors, and T. Petru, "Modeling and experimental verification of grid interaction of a DFIG wind turbine," IEEE Trans. Energy Convers., vol. 20, no. 4, pp. 878–886, Dec. 2005.
- [5] J. Lopez, E. Gubia, E. Olea, J. Ruiz, and L. Marroyo, "Ride through of wind turbines with doubly fed induction generator under symmetrical voltage dips," IEEE Trans. Ind. Electron., vol. 56, no. 10, pp. 4246–4254, Oct. 2009.
- [6] G. Pannell, D. J. Atkinson, and B. Zahawi, "Minimum-threshold crowbar for a fault-ride-through grid-code-compliant DFIG wind turbine," IEEE Trans. Energy Convers., vol. 25, no. 3, pp. 750–759, Sep. 2010.
- [7] A. O. Ibrahim, N. Thanh-Hai, L. Dong-Choon, and K. Su-Chang, "A fault ride-through technique of DFIG wind turbine systems using dynamic voltage restorers," IEEE Trans. Energy Convers., vol. 26, no. 3, pp. 871–882, Sep. 2011.
- [8] C. Wessels, F. Gebhardt, and F. W. Fuchs, "Fault ride-through of a DFIG wind turbine using a dynamic voltage restorer during symmetrical and asymmetrical grid faults," IEEE Trans. Power Electron., vol. 26, no. 3, pp. 807–815, Mar. 2011.
- [9] Y. Xiangwu, G. Venkataramanan, P. S. Flannery, W. Yang, D. Qing, and Z. Bo, "Voltage-sag tolerance of DFIG wind turbine with a series grid side passive-impedance network," IEEE Trans. Energy Convers., vol. 25, no. 4, pp. 1048–1056, Dec. 2010.
- [10] Y. Xiangwu, G. Venkataramanan, W. Yang, D. Qing, and Z. Bo, "Gridfault tolerant operation of a DFIG wind turbine generator using a passive resistance network," IEEE Trans. Energy Convers., vol. 26, no. 10, pp. 2896–2905, Oct. 2011.
- [11] P. S. Flannery and G. Venkataramanan, "A fault tolerant doubly fed induction generator wind turbine using a parallel grid side rectifier and series grid side converter," IEEE Trans. Power Electron., vol. 23, no. 3, pp. 1126–1135, May 2008.
- [12] P. S. Flannery and G. Venkataramanan, "Unbalanced voltage sag ride-through of a doubly fed induction generator wind turbine with series grid side converter," IEEE Trans. Ind. Appl., vol. 45, no. 5, pp. 1879–1887, Sep./Oct. 2009.
- [13] G. Pannell, B. Zahawi, D. J. Atkinson, and P. Missailidis, "Evaluation of the performance of a DC-Link brake chopper as a DFIG low-voltage fault-ride-through device," IEEE Trans. Energy Convers., vol. 28, no. 3, pp. 535–542, Sep. 2013.
- [14] M. Mohseni, S. Islam, and M. A. S. Masoum, "Fault ride-through capability enhancement of doubly-fed induction wind generators," IET Renew. Power Gener., vol. 5, no. 5, pp. 368–376, Sep. 2011.
- [15] M. Mohseni and S. M. Islam, "Transient control of DFIG-based wind power plants in compliance with the Australian grid code," IEEE Trans. Power Electron., vol. 27, no. 6, pp. 2813–2824, Jun. 2012.
- [16] X. Dongliang, X. Zhao, Y. Lihui, J. Ostergaard, X. Yusheng, and W. Kit Po, "A comprehensive LVVRT control strategy for DFIG wind turbines with enhanced reactive power support," IEEE Trans. Power Syst., vol. 28, no. 3, pp. 3302–3310, Aug. 2013.
- [17] Y. Lihui, X. Zhao, J. Ostergaard, D. Zhao Yang, and W. Kit Po, "Advanced control strategy of DFIG wind turbines for power system fault ride through," IEEE Trans. Power Syst., vol. 27, no. 2, pp. 713–722, May 2012.
- [18] J. Lopez, E. Gubia, P. Sanchis, X. Roboam, and L. Marroyo, "Wind turbines based on doubly fed induction generator under asymmetrical voltage dips," IEEE Trans. Energy Convers., vol. 23, no. 1, pp. 321–330, Mar. 2008.
- [19] X. Dawei, L. Ran, P. J. Tavner, and S. Yang, "Control of a doubly fed induction generator in a wind turbine during grid fault ride-through," IEEE Trans. Energy Convers., vol. 21, no. 3, pp. 652–662, Sep. 2006.
- [20] H. Sheng, L. Xinchun, K. Yong, and Z. Xudong, "An improved lowvoltage ride-through control strategy of doubly fed induction generator during grid faults," IEEE Trans. Power Electron., vol. 26, no. 12, pp. 3653–3665, Dec. 2011.
- [21] X. Shuai, Y. Geng, Z. Honglin, and G. Hua, "An LVVRT control strategy based on flux linkage tracking for DFIG-based WECS," IEEE Trans. Ind. Electron., vol. 60, no. 7, pp. 2820–2832, Jul. 2013.
- [22] G. Hua, L. Cong, and Y. Geng, "LVVRT capability of DFIG-based WECS under asymmetrical grid fault condition," IEEE Trans. Ind. Electron., vol. 60, no. 6, pp. 2495–2509, Jun. 2013.



ISSN (Print) : 2320 – 3765
ISSN (Online): 2278 – 8875

International Journal of Advanced Research in Electrical, Electronics and Instrumentation Engineering

(An ISO 3297: 2007 Certified Organization)

Vol. 4, Issue 12, December 2015

- [23] H. S. Song and K. Nam, "Dual current control scheme for PWM converter under unbalanced input voltage conditions," *IEEE Trans. Ind. Electron.*, vol. 46, no. 5, pp. 953–959, Oct. 1999.
- [24] L. Xu and Y. Wang, "Dynamic modeling and control of DFIG based wind turbines under unbalanced network conditions," *IEEE Trans. Power Syst.*, vol. 22, no. 1, pp. 314–323, Feb. 2007.
- [25] J. B. Hu, Y. K. He, and H. Nian, "Enhanced control DFIG-used back-to-back PWM VSC under unbalanced grid voltage conditions," *J. Zhejiang Univ. Sci. A*, vol. 8, no. 8, pp. 1330–1339, Aug. 2007.
- [26] M. Liserre, R. Teodorescu, and F. Blaabjerg, "Multiple harmonics control for three-phase grid converter systems with the use of PI-RES current controller in a rotating frame," *IEEE Trans. Power Electron.*, vol. 21, no. 3, pp. 1–6, May 2006.
- [27] R. Teodorescu et al., "Proportional-resonant controllers and filters for grid-connected voltage-source converters," *Proc. Inst. Elect. Eng.—Elect. Power Appl.*, vol. 153, no. 5, pp. 750–762, Sep. 2006.
- [28] I. Etxeberria-Otadui, A. Lopez De Heredia, H. Gaztanaga, S. Bacha, and M. R. Reyero, "A single synchronous frame hybrid (SSFH) multi frequency controller for power active filters," *IEEE Trans. Ind. Electron.*, vol. 53, no. 5, pp. 1640–1648, Oct. 2006.
- [29] J. B. Hu and Y. K. He, "Multi-Frequency Proportional-Resonant (MFPR) current controller for PWM VSC under unbalanced supply conditions," *J. Zhejiang Univ. Sci. A*, vol. 8, no. 10, pp. 1527–1531, Oct. 2007.
- [30] G. Escobar, A. M. Stankovic, and P. Mattavelli, "An adaptive controller in stationary reference frame for D-statcom in unbalanced operation," *IEEE Trans. Ind. Electron.*, vol. 51, no. 2, pp. 401–409, Apr. 2004.
- [31] G. Escobar, P. Mattavelli, A. M. Stankovic, A. A. Valdez, and J. Leyva-Ramos, "An adaptive control for UPS to compensate unbalance and harmonic distortion using a combined capacitor/load current sensing," *IEEE Trans. Ind. Electron.*, vol. 54, no. 2, pp. 839–847, Apr. 2007.